ELSEVIER

Journal of Computational and Applied Mathematics 126 (2000) 185–205

JOURNAL OF COMPUTATIONAL AND APPLIED MATHEMATICS

www.elsevier.nl/locate/cam

Contaminant dispersion from an elevated time-dependent source

B.S. Mazumder[a,*], D.C. Dalal[b]

[a] *Physics and Applied Mathematics Unit, Indian Statistical Institute, 203 B.T. Road, Calcutta 700 035, India*
[b] *Department of Mathematics, Indian Institute of Technology, Panbazar, Guwahati 781 001, India*

Received 2 March 1999; received in revised form 6 October 1999

Abstract

The release of waste materials from chemical plants or industries into a river or the atmosphere over a period of time is a common phenomenon. So the dispersion of contaminants for a time-dependent release is an important problem in controlling pollution. The present paper examines the streamwise dispersion of passive contaminant released from a time periodic source in a fully developed turbulent flow. A finite difference implicit method has been used to solve the unsteady convective diffusion equation employing a combined scheme of central and 4-point upwind differences. It is shown how the mixing of concentration of solute is influenced by the logarithmic velocity, the eddy diffusivities and the frequency of oscillatory release. The behaviour of iso-concentration lines in the vertical plane along the centreline due to the combined effect of velocity and turbulent diffusion has been examined for low and high frequencies of injection. The problem has been studied for time periodic continuous line and point sources. The concentration profiles for the steady elevated sources agree well with the existing experimental data. It has been observed that for low frequency, the iso-concentration lines become elongated without any oscillation in concentration in the longitudinal direction, whereas for higher frequency, the contours show a decaying oscillatory nature in concentration distribution along the downstream direction. The essential differences between dispersion from injection heights near the boundary and those away from the boundary are explained in terms of the relative importance of convection and eddy diffusion.

Keywords: Dispersion; Turbulent flow; Line sources; Point sources; Oscillatory injection; Numerical solution

1. Introduction

The dispersion of passive contaminant from an elevated source in a turbulent flow is worth studying from a practical viewpoint because of its application in environmental problems. In practice, the processes controlling the dispersion of dissolved and suspended pollutants in natural flows are numerous and complicated. In a real-world problem, the release of waste materials from chemical or industrial plants into a river or the atmosphere over a period of time is not at a constant rate.

* Corresponding author.
E-mail address: bijoy@isical.ac.in (B.S. Mazumder).

0377-0427/00/$ - see front matter
PII: S0377-0427(99)00353-2

Even in experiments on dispersion, it is extremely difficult to inject solute into a statistically steady flow at a constant rate. This fact supports the study of the present problem, namely dispersion from a time-dependent source into a known turbulent flow. This provides a better understanding of the basic scientific problems in predicting dispersion in more realistic situations, e.g., the time-dependent release of out-falls from chemical plants in rivers and canals [7], arbitrary release of smoke and inflammable gases from an elevated source in the atmosphere [4].

The longitudinal dispersion of soluble matter in a viscous liquid flowing through a circular pipe under turbulent conditions was discussed by Taylor [17] in his classic paper. To estimate the effect of longitudinal dispersion in turbulent diffusion, he assumed the coefficient of longitudinal diffusion to be equal to the coefficient of lateral diffusion. Taylor found that the centre of mass of the material has a velocity asymptotically equal to the discharge velocity and that the effect of longitudinal turbulent diffusion is very small. Elder [5] extended the study of Taylor to describe the dispersion in turbulent flow in an open channel. He performed a series of experiments to measure the longitudinal dispersion and showed that the contribution is approximately 2% of the main dispersion value. Carrier [2] studied the longitudinal dispersion of a solute concentration in a steady flow through a pipe when the distribution of concentration is prescribed as a harmonic function of time at a fixed cross-section of the pipe. Chatwin [3] made a study on longitudinal dispersion in a flow through a pipe when dispersion varies harmonically with time and developed methods for determining the transported speed of concentration and decay distance taking high and low frequency approximations for two simple parallel flows. He neglected the axial molecular diffusion coefficient and showed that for large value of frequency parameter $\omega a/u_*$ (a, ω and u_* are pipe radius, oscillation frequency and friction velocity, respectively), the concentration pattern is transported downstream at maximum rate and it takes place near the centre of the pipe. Barton [1] investigated the longitudinal dispersion of passive contaminants in parallel flows when the distribution of injected material was varying over a period of time. Taking a Fourier-transform in time, a non-standard eigenvalue problem was solved numerically to determine the concentration pattern, discharge speed and its decay distance downstream. In his analytical study, he considered dispersion in laminar flows neglecting longitudinal diffusion and also used a perturbation expansion for weak longitudinal diffusion, whereas for the case of turbulent channel flow he neglected the longitudinal diffusion. Plumb et al. [10] performed an experiment injecting oxygen as a contaminant for 20 min into the carrier gas (helium) which was flowing at about 10 m/s to study the effects of time-dependent input on the oxygen distribution. They showed from the experiment that if the dispersion of gas species at low pressure is considered, the axial molecular diffusion cannot be neglected. Dispersion from a time-dependent release of solute in parallel flows was also investigated by Smith [12] considering the input strength as a distribution of δ-function. He presented asymptotic solutions at small and large distances downstream from the source. Mazumder and Xia [9] presented an analytical solution for the longitudinal dispersion of pollutants in an asymmetric flow through a 2-D channel. Their analytical solutions were restricted to the cases when (i) the concentration of the injected material was initially uniform over the cross-section and (ii) the concentration varied harmonically with time at a certain cross-section of the channel.

Our main objective of the present paper is to explore the dispersion phenomenon of a solute injected from time-dependent continuous sources in a fully developed turbulent flow. More precisely, we study here how the injected material spreads when the release is periodic in time and also how the spreading of tracers is influenced by high and low frequency of pulsation. This problem may

be considered as a more realistic study of dispersion of pollutants in river, stream or atmospheric environments when the release of contaminant varies periodically with time. We have studied this problem for two cases as follows:

(i) Dispersion of contaminant from an elevated line source neglecting the cross-stream diffusion coefficient and considering the problem to be two-dimensional.
(ii) Dispersion of contaminant from an elevated point source and considering the problem to be three-dimensional where cross-stream diffusion coefficient has been taken into account.

A numerical scheme has been adopted to solve the convective–diffusion equation employing a combined scheme of central difference and 4-point upwind difference. Results have been discussed in the form of iso-concentration contours in the vertical plane for various frequencies and phases. The vertical concentration profiles resulting from the steady elevated line source agree well with the experimental data of Raupach and Legg [11], and the results from the solution-scheme of Sullivan and Yip [14]. Results due to the steady elevated point source have also been compared with the experimental data from Fackrell and Robins [6] and they also agree well. Sullivan and Yip [15,16] made a considerable improvement in the results near the source by introducing a time-dependent eddy diffusivity in the solution scheme. The present numerical scheme shows a better agreement with the experimental data away from the source.

2. Mathematical formulation

Let us consider a steady fully developed unidirectional turbulent flow of depth H, in which we employ a Cartesian coordinate system with origin at the bed surface ($z = 0$), x-axis along the flow, y-axis along cross-stream direction and z-axis perpendicular to the flow. If a slug is released over a period of time into the above-mentioned flow and the turbulent diffusion coefficients of the slug vary only with the vertical coordinate, the concentration $S(t,x,y,z)$ of the solute satisfies the dimensionless convective–diffusion equation of the form

$$\frac{\partial S}{\partial t} + u\frac{\partial S}{\partial x} = k_x(z)\frac{\partial^2 S}{\partial x^2} + k_y(z)\frac{\partial^2 S}{\partial y^2} + \frac{\partial}{\partial z}\left(k_z(z)\frac{\partial S}{\partial z}\right) \tag{1}$$

where $u = u^*/u_*$, $t = t^*u_*/H$, $z = z^*/H$, $x = x^*/H$, $y = y^*/H$, $k_{ij}(z) = k^*_{ij}/u_*H$.

Here u_* is the friction velocity and $k_{ij}(z)$ is the non-dimensional form of turbulent diffusivity tensor of the solute k^*_{ij}. (Here $k_{11} = k_x$, $k_{22} = k_y$ and $k_{33} = k_z$.) u,t,z,y,x are the dimensionless form of u^* (velocity of carrier fluid), t^* (time), z^*, y^*, x^*, respectively. H represents the depth of carrier fluid.

Effects of the off-diagonal terms in the eddy diffusivity tensor k_{ij} are found to be significant only at small times for individual clouds and these terms are not important for large time [13]. In this study, the off-diagonal terms in k_{ij} have been excluded in Eq. (1) as a continuous source has been considered.

The dimensionless boundary conditions of the problem are

$$\begin{aligned} &k_z(z)\left.\frac{\partial S}{\partial z}\right|_{z=0,1} = 0,\\ &S(\pm\infty, y, z, t) = 0,\\ &S(x, \pm\infty, z, t) = 0. \end{aligned} \tag{2}$$

The dispersion of pollutant is discussed when the injected material at the section ($x = 0,\ y = 0$) is initially prescribed as a harmonic function of time, and it is assumed that the concentration S at $x = 0,\ y = 0$ is of the form

$$S(0,0,z,t) = \delta(z - z_s)[1 + \exp(\mathrm{i}\omega t)], \tag{3}$$

where z_s is the height of injection point from the bottom, $\delta(z - z_s)$ is the Dirac delta function and $\omega(= \omega^* H/u_*)$ is the dimensionless frequency parameter.

The general form of the solution of Eq. (1) can be expressed as

$$S(x,y,z,t) = S_0(x,y,z) + S_1(x,y,z)\exp(\mathrm{i}\omega t), \tag{4}$$

where the first term on the right-hand side of (4) corresponds to the steady part and second part corresponds to the unsteady part of the concentration. Here, of course, the physical significance is attributed to the real part only.

Using (4) in Eqs. (1)–(3), and equating the coefficient of $\exp(\mathrm{i}\omega t)$ the equations become

$$u(z)\frac{\partial S_0}{\partial x} = k_x(z)\frac{\partial^2 S_0}{\partial x^2} + k_y(z)\frac{\partial^2 S_0}{\partial y^2} + \frac{\partial}{\partial z}\left(k_z(z)\frac{\partial S_0}{\partial z}\right), \tag{5}$$

$$\mathrm{i}\omega S_1 + u(z)\frac{\partial S_1}{\partial x} = k_x(z)\frac{\partial^2 S_1}{\partial x^2} + k_y(z)\frac{\partial^2 S_1}{\partial y^2} + \frac{\partial}{\partial z}\left(k_z(z)\frac{\partial S_1}{\partial z}\right) \tag{6}$$

subject to the boundary conditions

$$\begin{aligned} &S_0(\pm\infty, y, z) = 0 = S_0(x, \pm\infty, z),\\ &k_z(z)\frac{\partial S_0}{\partial z} = 0 \quad \text{at } z = 0, 1,\\ &S_0(0,0,z) = \delta(z - z_s) \end{aligned} \tag{7}$$

and

$$\begin{aligned} &S_1(\pm\infty, y, z) = 0 = S_1(x, \pm\infty, z),\\ &k_z(z)\frac{\partial S_1}{\partial z} = 0 \quad \text{at } z = 0, 1,\\ &S_1(0,0,z) = \delta(z - z_s). \end{aligned} \tag{8}$$

The solution of (5) subject to the boundary conditions (7) corresponds to steady-state dispersion. From Eq. (6), it can be easily stated that the unsteady part S_1 is a complex function. So the unsteady part S_1 can be written as the sum of in-phase and out-of-phase components in the form

$$S_1(x,y,z) = S_{1\mathrm{r}}(x,y,z) + \mathrm{i}S_{1\mathrm{i}}(x,y,z), \tag{9}$$

where $S_{1\mathrm{r}}$ and $S_{1\mathrm{i}}$ are real and imaginary parts of $S_1(x,y,z)$, respectively. Substituting the form of $S_1(x,y,z)$ from (9) into (6) and (8), and separating the real and imaginary parts one gets

$$-\omega S_{1\mathrm{i}} + u\frac{\partial S_{1\mathrm{r}}}{\partial x} = k_x(z)\frac{\partial^2 S_{1\mathrm{r}}}{\partial x^2} + k_y(z)\frac{\partial^2 S_{1\mathrm{r}}}{\partial y^2} + \frac{\partial}{\partial z}\left(k_z(z)\frac{\partial S_{1\mathrm{r}}}{\partial z}\right), \tag{10}$$

$$\omega S_{1\mathrm{r}} + u\frac{\partial S_{1\mathrm{i}}}{\partial x} = k_x(z)\frac{\partial^2 S_{1\mathrm{i}}}{\partial x^2} + k_y(z)\frac{\partial^2 S_{1\mathrm{i}}}{\partial y^2} + \frac{\partial}{\partial z}\left(k_z(z)\frac{\partial S_{1\mathrm{i}}}{\partial z}\right). \tag{11}$$

The pertinent boundary conditions are

$$\begin{aligned} &S_{1r}(\pm\infty, y, z) = S_{1i}(\pm\infty, y, z) = 0,\\ &S_{1r}(x, \pm\infty, z) = S_{1i}(x, \pm\infty, z) = 0,\\ &k_z(z)\frac{\partial S_{1r}}{\partial z} = k_z(z)\frac{\partial S_{1i}}{\partial z} = 0 \quad \text{at } z = 0, 1\\ &S_{1r}(0, 0, z) = \delta(z - z_s), \quad S_{1i}(0, 0, z) = 0 \end{aligned} \tag{12}$$

Here $S_0(x, y, z)$ and the real part of $S_1(x, y, z)\exp(i\omega t)$ represent the steady and unsteady parts of concentration distribution of the injected solute, respectively. The aim of the analysis is to solve the system of equations (5), (10) and (11) subject to the given boundary conditions (7) and (12).

3. Numerical procedure

In order to discuss the dispersion phenomena from the time-dependent release in turbulent flow, the system of equations (5), (10) and (11) with the boundary conditions (7) and (12) have been solved numerically using a finite difference technique. In using the numerical scheme, it is not convenient to incorporate boundary conditions at infinity. To resolve this problem along x and y, a transformation is taken to map the unbounded region (physical plane of (x, y, z) coordinate) to a bounded one (computational plane of (ξ, ζ, η) coordinate). The transformation used in this problem is of the form

$$x = \frac{1}{2a}\ln\left(\frac{1+\xi}{1-\xi}\right), \quad y = \frac{1}{2b}\ln\left(\frac{1+\zeta}{1-\zeta}\right) \quad \text{and} \quad z = \eta \tag{13}$$

for $-1 \leqslant \xi \leqslant 1,\ -1 \leqslant \zeta \leqslant 1,\ 0 \leqslant \eta \leqslant 1$.

Here a and b are the stretching factors. While going back to the physical plane from the computational plane one can extend the physical domain by choosing suitable values of a and b. It is clear from the relations that these parameters are inversely proportional to x and y for fixed grid lengths.

Let the transformed form of $u(z), k_x(z), k_y(z), k_z(z), S_0(z), S_{1r}(z)$ and $S_{1i}(z)$ be $\bar{u}(\eta), \bar{k}_x(\eta), \bar{k}_y(\eta), \bar{k}_z(\eta)$, $\bar{S}_0(\eta), \bar{S}_{1r}(\eta)$ and $\bar{S}_{1i}(\eta)$. But for convenience bars have been omitted.

Using the transformation (13), Eqs. (5), (10), (11) together with the boundary conditions (7) and (12) can be written, in the computational plane, as

$$\begin{aligned} &k_x a^2(1-\xi^2)\left\{(1-\xi^2)\frac{\partial^2 S_0}{\partial \xi^2} - 2\xi\frac{\partial S_0}{\partial \xi}\right\} + k_y b^2(1-\zeta^2)\left\{(1-\zeta^2)\frac{\partial^2 S_0}{\partial \zeta^2} - 2\zeta\frac{\partial S_0}{\partial \zeta}\right\}\\ &\quad + \frac{\partial}{\partial \eta}\left(k_z\frac{\partial S_0}{\partial \eta}\right) - ua(1-\xi^2)\frac{\partial S_0}{\partial \xi} = 0, \end{aligned} \tag{14}$$

$$\begin{aligned} &k_x a^2(1-\xi^2)\left\{(1-\xi^2)\frac{\partial^2 S_{1r}}{\partial \xi^2} - 2\xi\frac{\partial S_{1r}}{\partial \xi}\right\} + k_y b^2(1-\zeta^2)\left\{(1-\zeta^2)\frac{\partial^2 S_{1r}}{\partial \zeta^2} - 2\zeta\frac{\partial S_{1r}}{\partial \zeta}\right\}\\ &\quad + \frac{\partial}{\partial \eta}\left(k_z\frac{\partial S_{1r}}{\partial \eta}\right) - ua(1-\xi^2)\frac{\partial S_{1r}}{\partial \xi} + \omega S_{1i} = 0, \end{aligned} \tag{15}$$

$$k_x a^2(1-\xi^2)\left\{(1-\xi^2)\frac{\partial^2 S_{1i}}{\partial\xi^2}-2\xi\frac{\partial S_{1i}}{\partial\xi}\right\}+k_y b^2(1-\zeta^2)\left\{(1-\zeta^2)\frac{\partial^2 S_{1i}}{\partial\zeta^2}-2\zeta\frac{\partial S_{1i}}{\partial\zeta}\right\}$$
$$+\frac{\partial}{\partial\eta}\left(k_z\frac{\partial S_{1i}}{\partial\eta}\right)-ua(1-\xi^2)\frac{\partial S_{1i}}{\partial\xi}-\omega S_{1r}=0 \tag{16}$$

with the boundary conditions

$$\begin{aligned}&S_0(\pm1,\zeta,\eta)=0=S_0(\xi,\pm1,\eta),\\&k_z(\eta)\frac{\partial S_0}{\partial\eta}=0\quad\text{at }\eta=0,1,\\&S_0(0,0,\eta)=\delta(\eta-z_s),\end{aligned} \tag{17}$$

$$\begin{aligned}&S_{1r}(\pm1,\zeta,\eta)=S_{1i}(\pm1,\zeta,\eta)=0,\\&S_{1r}(\xi,\pm1,\eta)=S_{1i}(\xi,\pm1,\eta)=0,\\&k_z(\eta)\frac{\partial S_{1r}}{\partial\eta}=k(\eta)\frac{\partial S_{1i}}{\partial\eta}=0\quad\text{at }\eta=0,1,\\&S_{1r}(0,0,\eta)=\delta(\eta-z_s),\quad S_{1i}(0,0,\eta)=0.\end{aligned} \tag{18}$$

In order to solve this system of equations, a combined scheme of central differencing and 4-point upwind differencing has been employed [8]. The diffusion terms have been discretized using central differencing technique but for the convective terms the 4-point upwind scheme has been adopted. Because of the oscillatory behaviour of the three-point central difference representation of the convective term of the steady convection–diffusion equation and due to the dissipative nature of the 2-point upwind scheme, a 4-point upwind representation of the convective term $u\partial S/\partial\xi$ is useful and produces less error [8]. So this scheme is more accurate. The 4-point upwind scheme gives a spread out concentration front with a slightly oscillatory behaviour but it produces less error than other simple schemes.

$S(i,j,k)$ indicates the value of S at ith grid point along the ξ-axis, the jth grid point along the ζ-axis and the kth grid point along the η-axis where $\Delta\xi$ and $\Delta\eta$ are the grid spacings along ξ and η direction respectively. Here $i=1$, $i=N+1$ correspond to $\xi=0$, $\xi=1$; $j=1$, $j=L+1$ correspond to $\zeta=-1$, $\zeta=1$ and $k=1$, $k=M+1$ correspond to $\eta=0$, $\eta=1$ respectively. N,L and M represent the maximum number of grid spacings respectively along ξ,ζ and η directions.

So the discretized form of $\partial S/\partial\xi$ at (i,j,k) grid point is given below.

For velocity $u>0$, the representation is

$$\left.\frac{\partial S}{\partial\xi}\right|_{ijk}=\frac{S(i+1,j,k)-S(i-1,j,k)}{2\Delta\xi}$$
$$+\frac{q(S(i-2,j,k)-3S(i-1,j,k)+3S(i,j,k)-S(i+1,j,k))}{3\Delta\xi}$$
$$+\mathrm{O}(\Delta\xi^2) \tag{19}$$

and for $u < 0$, it will be

$$\left.\frac{\partial S}{\partial \xi}\right|_{ijk} = \frac{S(i+1,j,k) - S(i-1,j,k)}{2\Delta\xi} + \frac{q(S(i-1,j,k) - 3S(i,j,k) + 3S(i+1,j,k) - S(i+2,j,k))}{3\Delta\xi} + \mathrm{O}(\Delta\xi^2). \tag{20}$$

The parameter q controls the size of the modification of the 3-point central finite difference formula and it is effective in reducing dispersion error. The suitable choice of q eliminates the $\Delta\xi^2\,\mathrm{d}^3S/\mathrm{d}\xi^3$ and makes Eqs. (19) or (20) of the order of $\Delta\xi^3$. So this, with the discretization of $\mathrm{d}^2S/\mathrm{d}\eta^2$ produces a more accurate solution. It has been observed that simple schemes including 3-point formula produce oscillatory solutions. On a finer grid, a suitable choice of q produces comparatively more accurate and nonoscillatory solutions.

As the flow is fully developed turbulent flow, convection along the horizontal direction will be much larger than the longitudinal diffusion of the solute. If the solute is injected at the line $\xi = 0$, it cannot reach the negative side of $\xi = 0$ line because of dominance of the convective effect. So the concentration of the solute for $-1 \leqslant \xi < 0$ can be assumed as zero. The grid point where the solute is injected is described as $(1, 1 + 1/\Delta\zeta, ks)$.

So the boundary conditions (17) and (18) for $\xi = 0$ and 1 can be written as

$$\begin{aligned}
&S_0(1, 1 + 1/\Delta\zeta, ks) = 1, \quad S_{1\mathrm{r}}(1, 1 + 1/\Delta\zeta, ks) = 1,\\
&S_0(1,j,k) = S_{1\mathrm{r}}(1,j,k) = 0 \quad \text{for } 0 \leqslant j \leqslant L+1,\ 0 \leqslant k \leqslant M+1 \text{ except } k = ks,\\
&S_{1\mathrm{i}}(1,j,k) = 0 \quad \text{for } 0 \leqslant j \leqslant L+1 \text{ and } 0 \leqslant k \leqslant M+1,\\
&S_0(N+1,j,k) = S_{1\mathrm{r}}(N+1,j,k) = S_{1\mathrm{i}}(N+1,j,k) = 0 \quad \text{for } 0 \leqslant k \leqslant M+1,\\
&S_0(i,L+1,k) = S_{1\mathrm{r}}(i,L+1,k) = S_{1\mathrm{i}}(i,L+1,k) = 0 \quad \text{for } 0 \leqslant k \leqslant M+1.
\end{aligned} \tag{21}$$

The following conditions have been incorporated for accurate and stable results:

$$\Delta\xi = \left.\frac{k_x(\eta)}{u(\eta)}\right|_{\min} \quad \forall i,j,k$$

and

$$q = \frac{1}{2}\left[1 + \frac{a\xi k_z(\eta)}{u(\eta)}\right].$$

We can take $\Delta\xi = \Delta\zeta/2 = \Delta\eta$.

An inverse transformation has been applied to go back from the computational plane to the physical plane and to obtain the desired results after solving the discretized system of algebraic equations using an Successive Over Relaxation (SOR) technique. The appropriate relaxation parameter has been chosen after numerical experimentation.

4. Discussion of results

In order to discuss results, the configurations of dimensionless velocity and eddy diffusivity are respectively taken, following Sullivan and Yip [14] as

$$u(z) = \frac{1}{2\kappa} \ln[(z/z_0)^2 + \exp(-(z/z_0)^2)] \tag{22}$$

and

$$k_x(z) = k_z = \kappa z_0 [C_0^2 (z_1/z_0)^2 + (z/z_0)^2]^{1/2}, \tag{23}$$

where κ is von Kármán constant $= 0.38$, z_0 is the roughness of the bottom of the channel, z_1 is the nominal size of gravel and constant $C_0 = 1.25$. The flow is considered to be bounded between $0 \leqslant z' \leqslant H$ and at the height $z' = H(z = 1)$ the velocity is maximum, i.e., the free-stream velocity.

The distributions (22) and (23) are different from the usual logarithmic velocity profile $u(z) = (1/\kappa)\ln(z/z_0)$ and the eddy diffusivity $k(z) = \kappa z$. Eq. (22) satisfies the no-slip condition at the bed and Eq. (23) represents the diffusivity over a thin region near the bed if the constant C_0 is equal to zero.

The transformed forms of (22) and (23) are

$$u(\eta) = \frac{1}{2\kappa} \ln[(\eta/z_0)^2 + \exp(-(\eta/z_0)^2)], \tag{24}$$

$$k_z(\eta) = z_0 \kappa [C_0^2 (z_1/z_0)^2 + (\eta/z_0)^2]^{1/2}. \tag{25}$$

The problem has been studied for two different cases: (i) two-dimensional (neglecting cross-stream diffusion k_y), when contaminant is injected from an elevated time-dependent line source placed at $\xi = 0$, and (ii) three-dimensional when cross-stream diffusion is considered and solute is injected for an elevated time-dependent point source placed at $\xi = 0$ and $\zeta = 0$.

4.1. Two-dimensional case

For two-dimensional case we have taken $k_x(\eta) = k_z(\eta)$ and $k_y(\eta) = 0.0$. To verify the accuracy of the scheme, results of the steady-state dispersion of the present problem have been compared with experimental and numerical data. Raupach and Legg [11] performed experiments on passive tracer dispersion from an elevated line source in a turbulent boundary layer to study the scalar concentration distribution. A rough surface was made by gluing gravel (nominal size of gravel is $z_1 = 7$ mm) to wooden base board in a wind tunnel and a heat source was placed at a height of $h = 60$ mm above the zero plane of the surface. The depth of the carrier fluid has been taken to be 0.54 m. Their measured data were found to provide an approximately logarithmic velocity profile $u = (u_*/\kappa)\ln(z/z_0)$ where the roughness height $z_0 = 0.12$ mm and the value of κ was 0.38 within the acceptable range. In our numerical study, we have used the velocity profile and diffusivity as Eqs. (22) and (23) with ($z_1 \neq 0$) and without ($z_1 = 0$) gravel in the bed surface and stretching factor $a = 0.05$. The steady part of the concentration S_0 has been computed at four different positions downstream from the source ($x/h = 2.5, 7.5, 15.0$ and 30.0) considering values of the other parameters the same as taken by Raupach and Legg [11], and Sullivan and Yip [14]. To provide a comparison

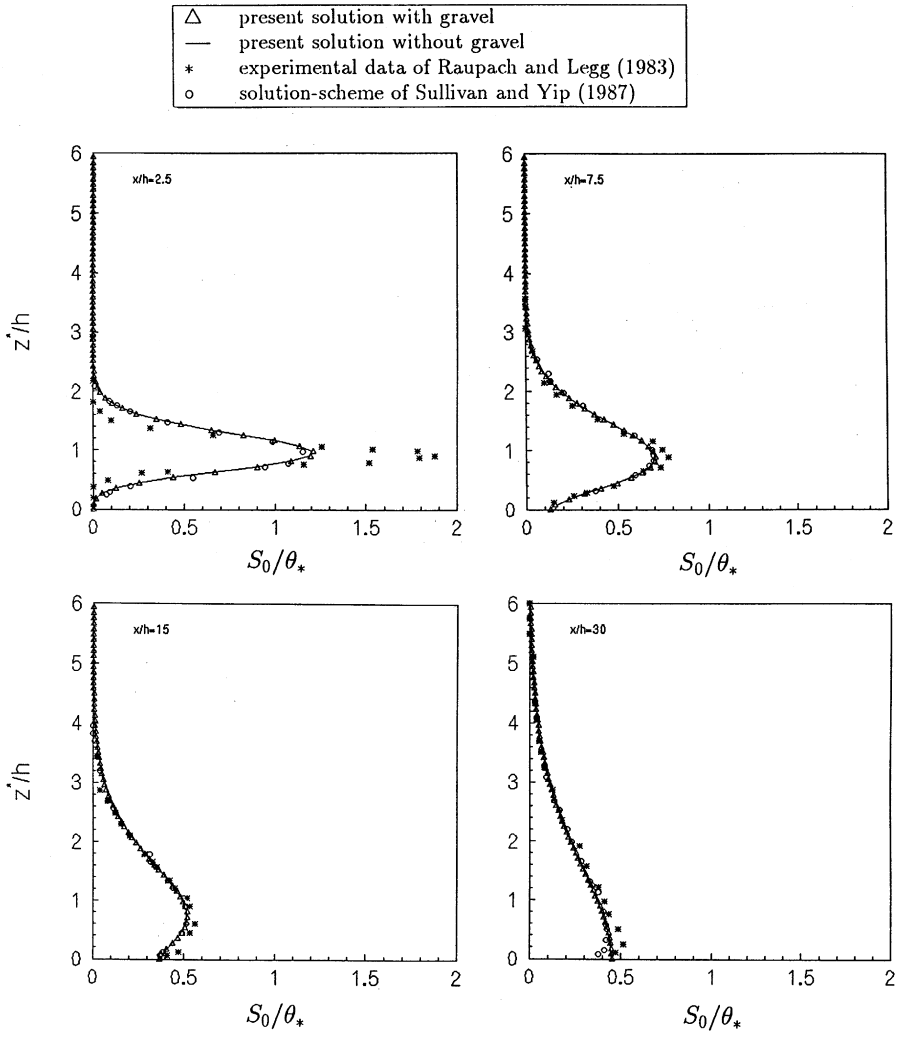

Fig. 1. A comparison between the dimensionless steady concentration profiles at various downstream distances.

with the experimental and computed values of concentration, following Raupach and Legg [11], concentration S_0 has been normalized by a scale θ_* of the form

$$\theta_* = \frac{F}{hu(h)}, \tag{26}$$

where F is the constant flux of contaminant normal to the flow.

Present results with and without gravel at the bed surface are compared with experimental data of Raupach and Legg [11] and the solution scheme of Sullivan and Yip [14], and shown in Fig. 1. From the figures, it is observed that the numerical results for the steady-state concentration S_0 are in good agreement with those of Raupach and Legg [11] and Sullivan and Yip [14]. It may also be noted from the concentration profiles that the effect of the gravel bed is not significant in the main flow except near the boundary.

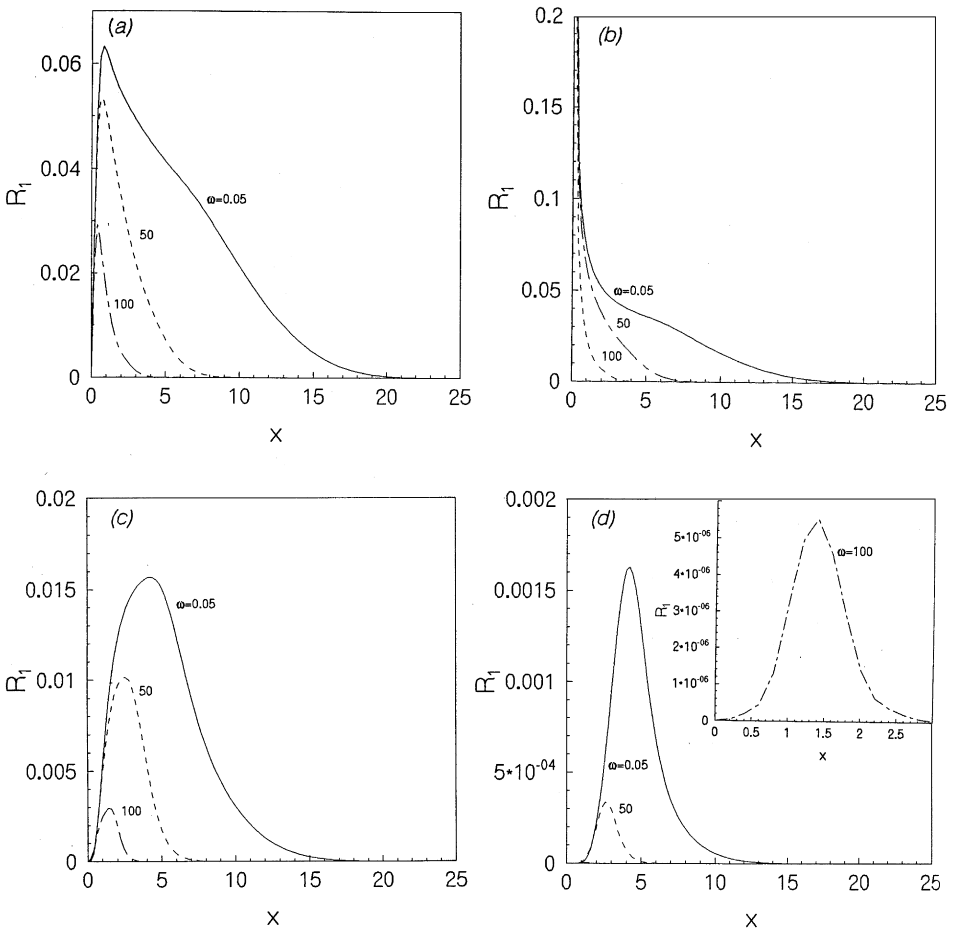

Fig. 2. The variation of amplitude R_1 of unsteady concentration at different heights along downstream when $z_s = 0.11$: (a) $z = 0.06$, (b) $z = 0.11$, (c) $z = 0.3$ and (d) $z = 0.6$.

In order to discuss the unsteady part of the solute concentration, we use the dimensionless frequency parameter $\omega = 2\pi(H/u_*)/T$, which is a measure of the ratio of the time (H/u_*) taken for transport of mixing of momentum and energy over the cross-section due to turbulent diffusion to the period of oscillation $(1/\omega^*)$. Thus the parameter $\omega^* H/u_*$ plays an important role in turbulent flow as does $\omega^* a^2/k$ in a laminar flow, where a is the radius of the pipe and k is constant molecular diffusivity. A small value of ω implies a large oscillation period compared with the turbulent diffusion time, and therefore, the nature of the flow is known as 'quasi-steady', and vice versa for large ω. The problem is considered here for two different heights of injection: (i) at height $z_s = 0.11$ near the boundary and (ii) $z_s = 0.6$ away from the boundary.

Fig. 2(a) shows the amplitude R_1 $(=\sqrt{S_{1r}^2 + S_{1i}^2})$ of the unsteady part S_1 of the solute concentration at a particular height $z = 0.06$ (which is below the point of injection) for different $\omega = 0.05, 50.0$ and 100.0. As the computation of amplitude is made below the injection point, initially the amplitude R_1 increases from zero along the downstream distance up to a certain value, then decreases to

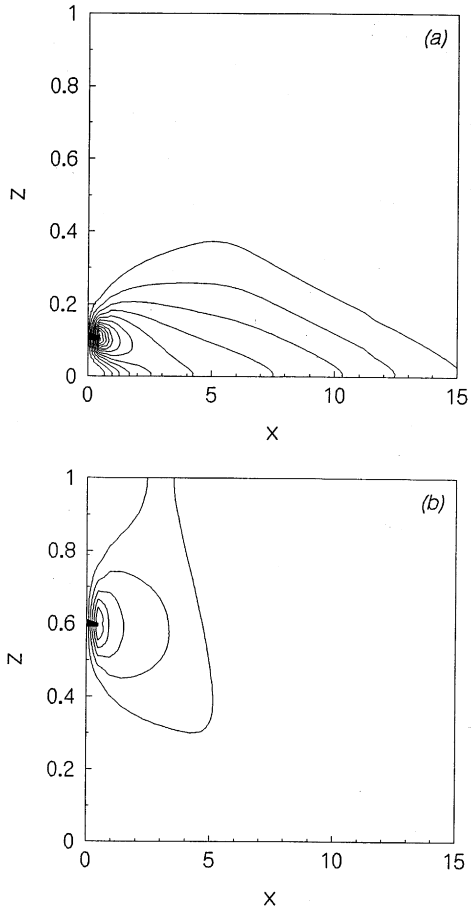

Fig. 3. Equi-concentration lines of steady part in a vertical plane: (a) when the slug is injected at $z_s = 0.11$ and (b) when it is injected at $z_s = 0.6$. Concentration value of the outermost contour is 0.01 and it increases with interval 0.01.

zero gradually. For the low frequency, concentration decreases to zero slowly along the streamwise direction but for the high frequency it decreases very fast. So with an increase of the frequency parameter ω the decay distance of concentration S_1 decreases. Fig. 2(b) presents the amplitude of concentration at the injection point at $z = 0.11$. It is also noted that amplitude of S_1 decreases on increase of x because of vertical and longitudinal turbulent diffusion and with the increase of frequency of pulsation. Figs. 2(c) and (d) show the variations of amplitude of S_1 along x for heights 0.3 and 0.6, respectively. The behaviour of the graphs are the same as that of Fig. 2(a) but the maximum value of the amplitude of S_1 decreases with height from the injection point and the difference between maximum values of R_1 for low and high frequencies also decreases with the increase of height. This observation can be compared with that of Chatwin [3]. Barton [1] has also mathematically shown that the decay distance of concentration is larger for low-frequency approximation than that for high frequency.

The lines of equi-concentration of the steady part of S in the vertical plane have been plotted in Fig. 3(a), when the solute is injected from a height $z_s = 0.11$ near the bottom and in Fig. 3(b),

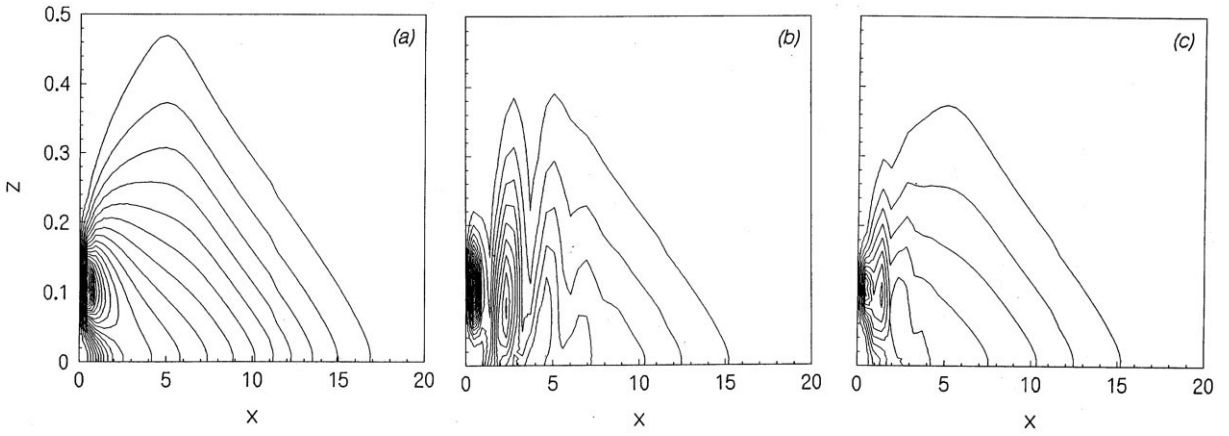

Fig. 4. Iso-lines of concentration (combined steady and unsteady) in a vertical plane when $\omega t = 0$ and slug is injected at a height $z_s = 0.11$: (a) $\omega = 0.05$, (b) $\omega = 50$ and (c) $\omega = 100$. Concentration value of the outermost contour is 0.01 and it increases with interval 0.01.

when it is injected from $z_s = 0.6$ away from the bottom. From the diagram it is observed that the contours of iso-concentration become more elongated longitudinally than that along the transverse direction because the dispersion due to longitudinal convection is more prominent than that due to vertical diffusion. The solute disperses in the both longitudinal and vertical directions due to the combined effect of shear and eddy diffusion. Fig. 3(a) also shows a slight tilting of the concentration contour towards the bottom, which may be due to the higher velocity gradient near the bed (turbulent boundary layer). As the velocity is low near the bed, the solute concentration in the lower velocity region disperses slowly, whereas in the higher velocity region, it disperses faster. But Fig. 3(b) shows the symmetric features of iso-concentration profile in the main flow upto some distance downstream, where the velocity gradient is low.

The variation of the equi-concentration lines of S (combining both the steady and unsteady parts, i.e., S_0 + real part of $S_1 \exp(i\omega t)$) in a vertical xz-plane for various values of frequency parameter ($\omega = 0.05, 50.0, 100.0$) have been plotted in Fig. 4. The computation is performed when the solute is injected near the bottom ($z_s = 0.11$) and phase $\omega t = 0$ (i.e., release is maximum). The contour for low frequency ($\omega = 0.05$) is almost similar with that of steady concentration, which may be designated as 'quasi-steady'. For a low frequency parameter ($\omega = 0.05$) it is seen from the Fig. 4(a) that the contours get more elongated in the longitudinal direction than the transverse, and the solute spreads very slowly near the bottom due to a low velocity there, whereas for higher frequency, the plume seems to be broken up into several patches along the downstream direction from the source though there is a continuity. The lateral dispersion of solute is oscillatory in nature. Near the source this oscillation is prominent and it dies out gradually in the downstream direction. As deduced by Chatwin [3] and Smith [12], we have reproduced the results that for low frequency there is a weaker variation of concentration across the flow. Due to the formation of small-scale eddies, the mixing process is more effective near the boundary and it destroys the oscillatory nature in concentration with increase in x. From Figs. 4(a)–(c) it is observed that the oscillatory nature in concentration away from the boundary is reflected properly along the downstream direction for the moderate value of frequency ω.

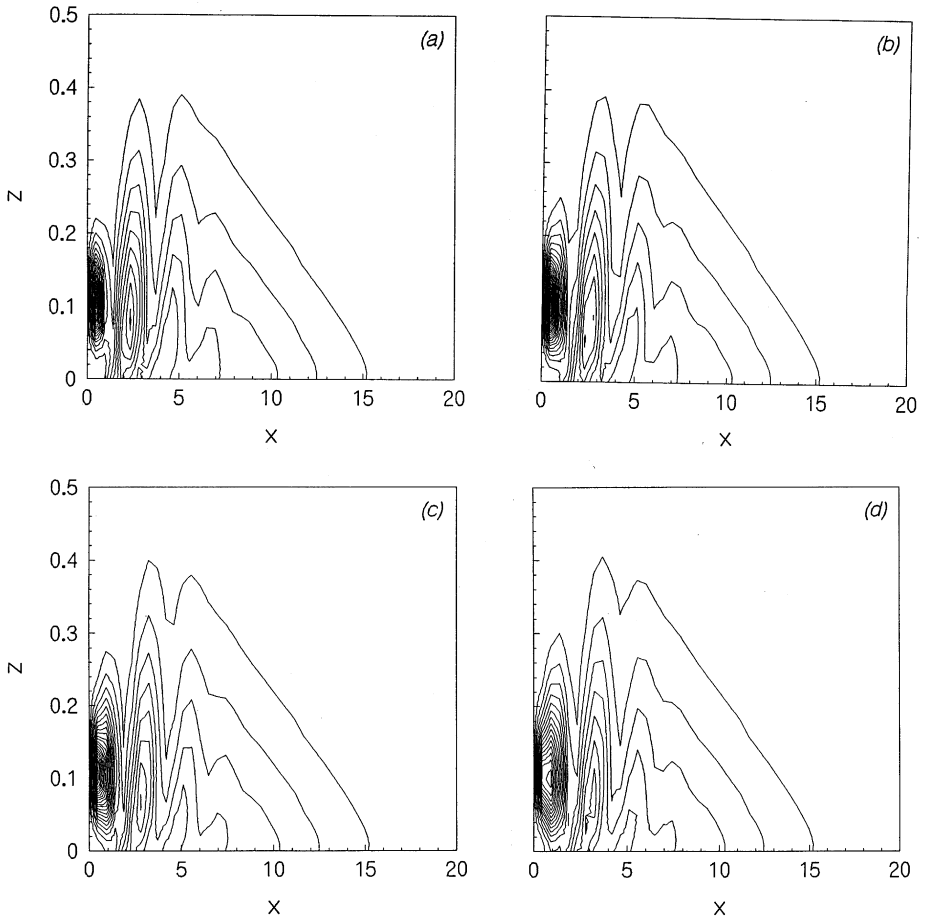

Fig. 5. Iso-lines of concentration (combined steady and unsteady) in a vertical plane when $\omega = 50$ and slug is injected at a height $z_s = 0.11$: (a) $\omega t = 0$, (b) $\omega t = \pi/4$, (c) $\omega t = \pi/2$ and (d) $\omega t = 3\pi/4$. Concentration value of the outermost contour is 0.01 and it increases with interval 0.01.

The computation has also been performed for the time of release at different phases ($\omega t = 0$, $\frac{1}{4}\pi$, $\frac{1}{2}\pi$ and $\frac{3}{4}\pi$). Figs. 5(a)–(d) show the instantaneous iso-concentration lines of S along the downstream for the frequency parameter $\omega = 50$ after the release of contaminant from the source. As the amount of release from the source is different for different phases, the dispersed area of concentration is also different, even if it is compared with the value of equi-concentration lines. It is important to note that although the time of release is different for fixed frequency, the behaviour of the iso-concentration contour is almost same for all cases.

To observe the effect of the point of injection, the solute is injected at the height $z_s = 0.6$ from the zero plane. Equi-concentration lines for low frequency ($\omega = 0.05$) as well as high frequency ($\omega = 50$) have been shown in Figs. 6(a) and (b) for $\omega t = 0$. As the velocity near the surface is greater, the convective effect will also be greater and if we compare the contour lines of Fig. 4(a) with those of Fig. 6(a), it is easily seen that the lines are vertically more dispersed in case of release of contaminant at $z_s = 0.6$ than the case of release near the bottom $z_s = 0.11$, and contours of the

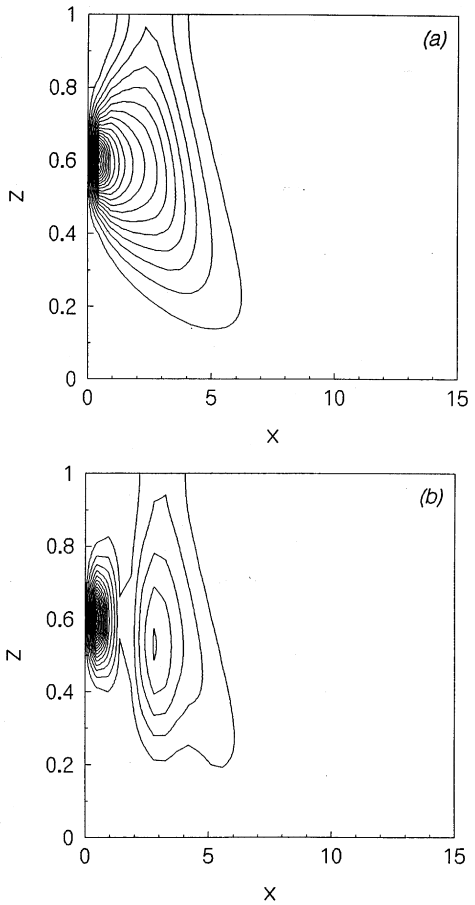

Fig. 6. Equi-concentration lines for combined steady and unsteady parts in a vertical plane for $\omega t = 0$: (a) $\omega = 0.05$ and (b) $\omega = 50$, when the slug is injected at $z_s = 0.6$. Concentration value of the outermost contour is 0.006 and it increases with interval 0.006.

first case are symmetrically elongated along the downstream. For high frequency, contour lines of Fig. 5(a) become wider than that of Fig. 6(b). It is seen from the Figs. 5(a) and 6(b) that the transverse diffusion effect for the source near the bottom is more significant than that away from the bottom because of sharp velocity gradient near the bottom wall. When a solute is released from a higher point (where boundary layer effect is not significant) the longitudinal dispersion is higher due to higher velocity. Therefore, at a fixed cross-section downstream, the surge of concentration arrives earlier and is much more symmetrical about the injection line at $z_s = 0.6$ and 0.11 near the bed [12]. Also it is observed that at a larger distances downstream from the source, there is more mixing across the flow.

4.2. Three-dimensional case

For the three-dimensional model (i.e., considering the cross-stream diffusion effect), results have been compared with the experimental data from Fackrell and Robins [6]. They performed an

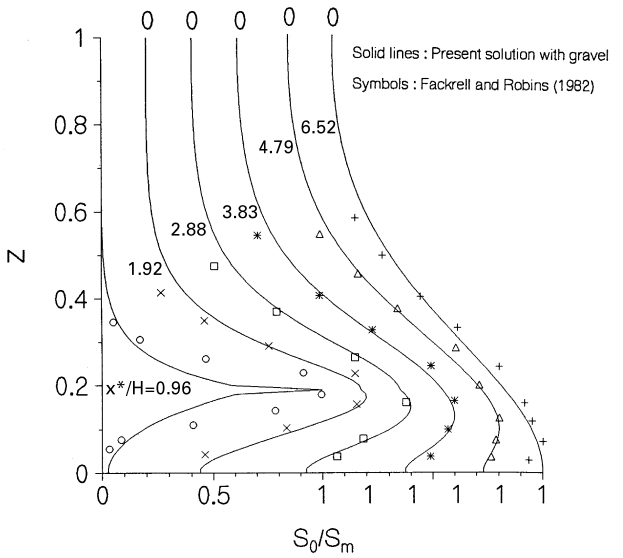

Fig. 7. A comparison between the experimental and theoretical vertical profiles of steady concentration at various distances from the source.

experiment for steady three-dimensional contaminant field where a continuous elevated point source was placed within a rough-walled wind tunnel boundary layer of height 1.2 m. The mean velocity profile has been taken the same as the previous case with following eddy diffusivity coefficients:

$$k_x(z) = k_y(z) = k_z(z). \tag{27}$$

The experiment was performed with a constant release of a contaminant from a height $z_s(=h/H) = 0.19$. Taking the velocity and diffusivity profiles (24) and (27), stretching factors $a = 0.01$, $b = 0.01$ along the ξ and ζ direction, respectively, and using values of the necessary parameters from Fackrell and Robins [6], vertical profiles of the steady part of concentration are computed at six different longitudinal positions ($x^*/H = 0.96, 1.92, 2.88, 3.83, 4.79$ and 6.52). The concentration profiles are normalized by the maximum concentration (S_m) in the plane at a particular distance from the source. Results are plotted in Fig. 7 together with the results of Fackrell and Robins [6]. It is observed that the numerical results for the steady part of concentration S_0 are in good agreement with those of Fackrell and Robin [6] for all downstream stations.

Figs. 8(a) and (b) show the iso-concentration lines of steady part in the vertical plane along central line of the channel (i.e., $y = 0$) when material is injected at $z_s = 0.11$ and $z_s = 0.6$ respectively. The patterns of iso-concentration lines are similar as those in Figs. 3(a) and (b). Realizing the same physics as discussed for Fig. 3, it is seen that when the solute injected near bottom, it accumulates near the wall upto a certain distance downstream but for the case (b), there is a symmetry in dispersion.

Figs. 9(a), (b), (c) show iso-concentration lines when release is maximum (i.e., phase $\omega t = 0$) from the point $z_s = 0.11$ for frequencies 0.05, 50 and 100, respectively, at the central vertical xz-plane (i.e., $y = 0$). The figures show that with an increase in frequency of oscillation, the oscillation in the concentration distribution is not significant. For small frequency, solute disperses more than that for higher frequency (Figs. 9(a) and (b)). The rate of change in higher frequency is not significant

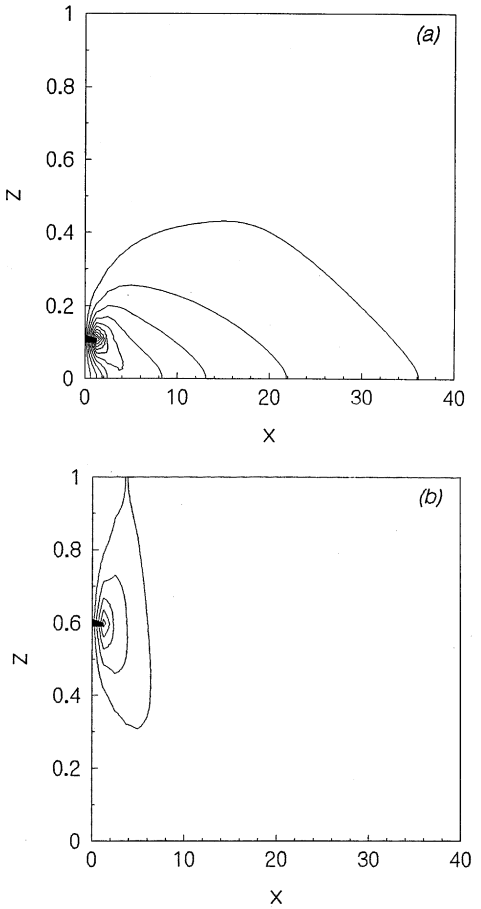

Fig. 8. Same as Fig. 3 with three-dimensional effect. Concentration value of the outermost contour is 0.01 and it increases with interval 0.01.

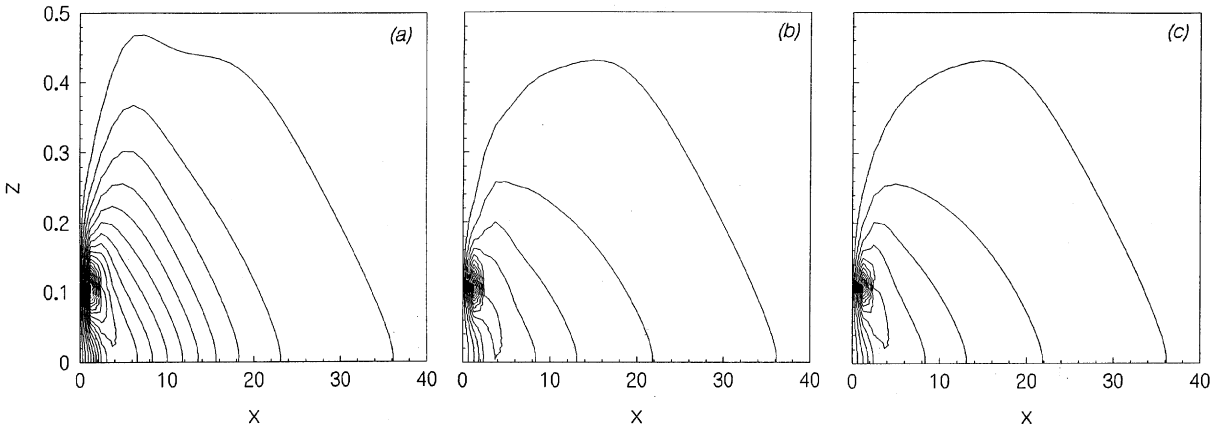

Fig. 9. Same as Fig. 4 with three-dimensional effect. Concentration value of the outermost contour is 0.01 and it increases with interval 0.01.

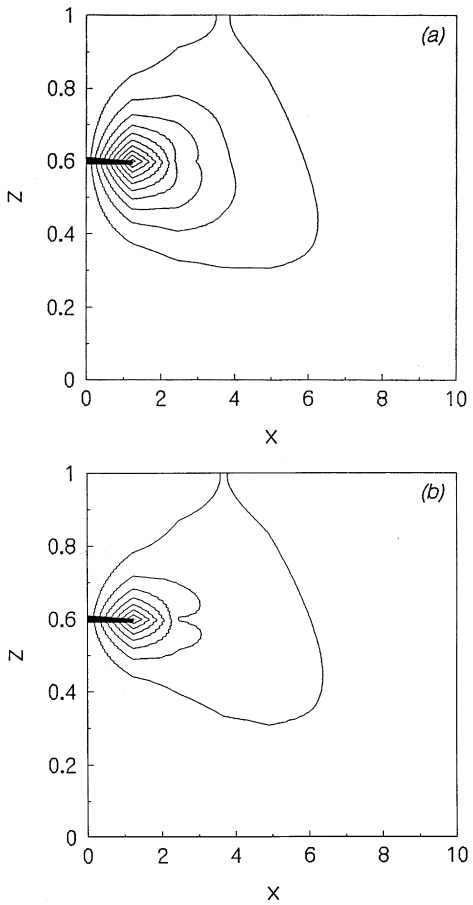

Fig. 10. Same as Fig. 6 with three-dimensional effect. Concentration value of the outermost contour is 0.01 and it increases with interval 0.01.

(Figs. 9(b) and (c)). This may be due to the formation of small-scale eddies of the turbulent velocity field near the lower wall are comparatively much more effective at mixing and decaying the oscillatory nature in concentration along downstream. From Figs. 10(a) and (b), this phenomenon may be more clear when the plume is injected at $z_s = 0.6$. As velocity gradient along z is not significant, plume diffuses symmetrically just after release. So for low frequency, it disperses faster than that for high frequency.

The effects of phase (i.e. the amount of released material) have been presented in Figs. 11(a)–(d) and it is revealed that the effects are not significant. Near the source, some changes are noticed. With changes of phase (0, $\frac{1}{4}\pi$, $\frac{1}{2}\pi$ and $\frac{3}{4}\pi$), the dispersion increases slightly in the near field but at far field there are no significant effects although the time of release is different for fixed frequency.

Diffusion of the injected materials for low frequency along cross-stream direction at different downstream positions ($x = 2.0, 5.0$ and 10.0) has been shown in Figs. 12(a)–(c) when the height of the point of injection is 0.11. Solute diffuses in the form of parabola instead of circle. This is due to the presence of boundary effects. Near the bottom, material diffuses more in the upward direction

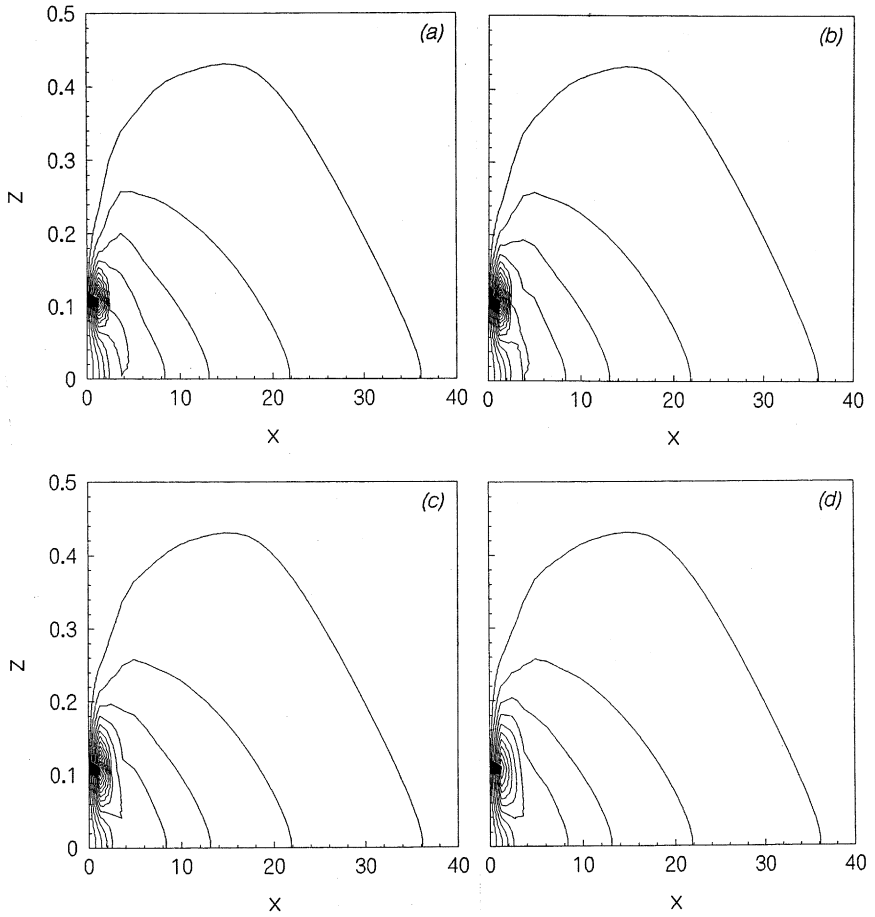

Fig. 11. Same as Fig. 5 with three-dimensional effect. Concentration value of the outermost contour is 0.01 and it increases with interval 0.01.

than that in the downward. As x increases along downstream, the slug spreads vertically due to differential convection. For large frequency ($\omega = 50$), Fig. 13(a) shows that the material diffuses much slowly near the source and oscillatory behaviours are reflected in the distribution of solution which can be seen from Fig. 12(a) but for far away, the effect of frequency is not significant as the oscillations decay with x. As the nature of injection is oscillatory, it persists near the source but when it moves towards the downstream direction it mixes with the fluid and gets diluted which causes to lose its oscillatory behaviour in the far field. If contaminant is released from a higher point (say $z_s = 0.6$) shown in Figs. 14(a)–(c), it disperses symmetrically near the source and then it diffuses downward with x.

5. Conclusions

The aim of this of paper is to explore the dispersion of passive contaminants in a turbulent flow due to the combined effect of logarithmic velocity and eddy diffusivities, when the distribution of

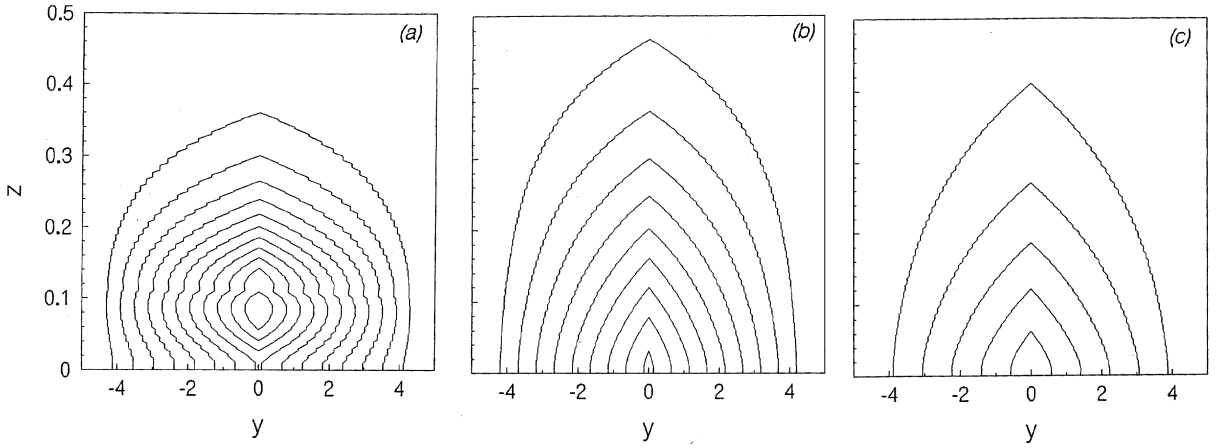

Fig. 12. Equi-concentration lines for combined steady and unsteady parts in a vertical plane (across the flow) at different downstream direction for $\omega t = 0$ and $\omega = 0.05$: (a) at $x = 2.0$, (b) at $x = 5.0$ and (c) at $x = 10.0$ when the slug is injected at $z_s = 0.11$. Concentration value of the outermost contour is 0.01 and it increases with interval 0.01.

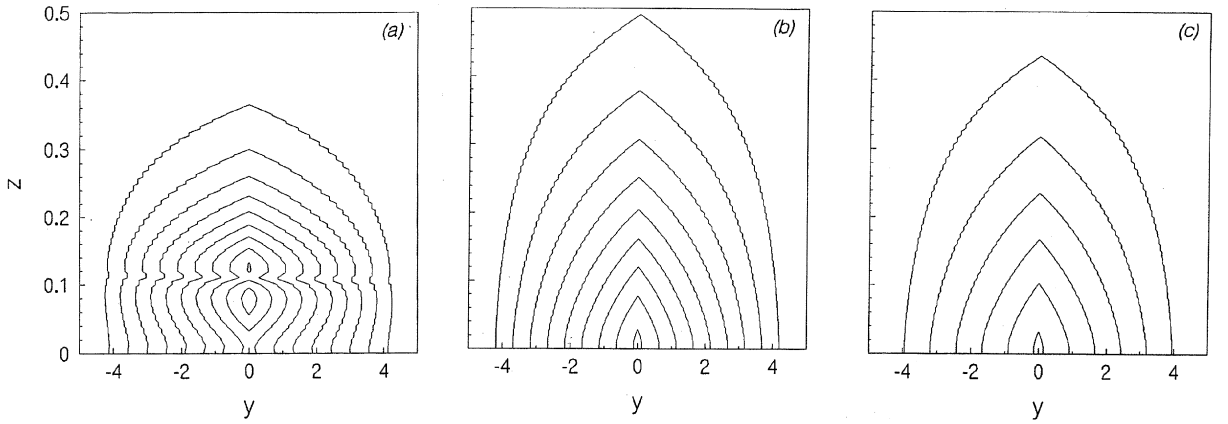

Fig. 13. Same as Fig. 12 for $\omega = 50.0$. Concentration value of the outermost contour is 0.005 and it increases with interval 0.005.

concentration across the flow ($x = 0$) is prescribed as a harmonic function of time. The transport equations have been solved numerically for a better understanding of the dispersion process when the injection of contaminant is oscillatory in nature. Calculations have been made over a gravel bed and compared with the experimental findings. It is worth mentioning that the effect of the gravel bed is not significant in the main flow except for a small effect near the boundary. Injection of material with low frequency does not much affect the nature of steady release whereas, with an increase of frequency, the oscillatory nature of injection gets reflected in the concentration distribution along the downstream distance. Along lateral direction there is an oscillation in concentration which is directly related to the injection frequency and fluctuations gradually decay downstream. Phase of release does not make any significant changes in nature of dispersion, near the source a small effect may be noticed. The height of injection changes significantly the pattern of dispersion. As the contaminant

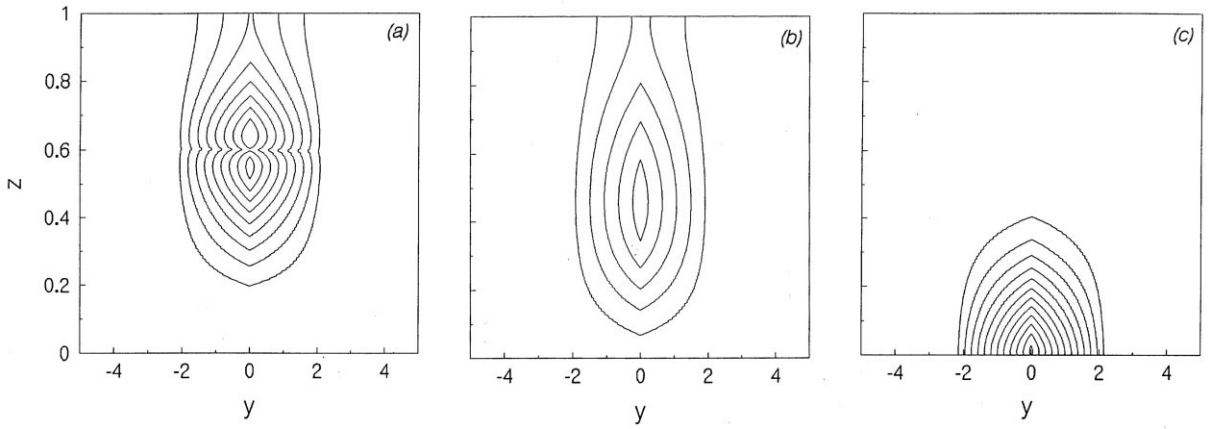

Fig. 14. Same as Fig. 13 when the slug is injected at $z_s = 0.6$. Concentration values of the outermost contour and increment are 0.002 for (a) and (b) and 0.0002 for (c).

moves faster for higher elevated source than for lower one, there is a tendency to develop an asymmetry in dispersion of material when it is injected near the bottom wall. This perhaps due to the formation of eddies near the wall which increases the mixing processes.

This problem could have been solved easily using the solution scheme proposed by Sullivan and Yip [13]. But if the problem is generalized by considering the effects of a second-order reaction in the flow, boundary retention, effect due to the presence of dead zones, etc., this scheme may not be useful unless it is modified accordingly. However, a more general problem can easily be solved employing the present numerical scheme.

Acknowledgements

The authors would like to express their sincere thanks to Professor P.J. Sullivan, Department of Applied Mathematics, University of Western Ontario, Canada for his helpful comments and suggestions for improvements of the paper.

References

[1] N.G. Barton, The dispersion of solute from time dependent releases in parallel flow, J. Fluid Mech. 136 (1983) 243–267.
[2] G.F. Carrier, On diffusive convection in tubes, Q. Appl. Math. 14 (1956) 108–112.
[3] P.C. Chatwin, On the longitudinal dispersion of dye whose concentration varies harmonically with time, J. Fluid Mech. 58 (1973) 657–667.
[4] G.T. Csanady, Turbulent Diffusion in the Environment, D. Reidel Publishing Company, Dordrecht, 1980.
[5] J.W. Elder, The dispersion of marked fluid in turbulent shear flow, J. Fluid Mech. 5 (1959) 544–560.
[6] J.E. Fackrell, A.G. Robins, Concentration fluctuations and fluxes in plumes from point sources in a turbulent boundary layer, J. Fluid Mech. 117 (1982) 1–26.
[7] H.B. Fischer, E.J. List, R.C.Y. Koh, J. Imberger, N.H. Brooks, Mixing in Inland and Coastal Waters, Academic Press, New York, 1979.

[8] C.A.J. Fletcher, Computational Techniques for Fluid Dynamics, Vol. 1, Springer, Berlin, 1988.
[9] B.S. Mazumder, R. Xia, Dispersion of pollutants in an asymmetric flow through a channel, Int. J. Engg Sci. 32 (1994) 1501–1510.
[10] I.C. Plumb, K.R. Ryan, N.G. Barton, A method for measurement of diffusion coefficients of labile gas phase species: the diffusion coefficient of $O(^3P)$ in He at 294 K, Int. J. Chem. Kinet. 15 (1983) 1081–1097.
[11] M.R. Raupach, B.J. Legg, Turbulent dispersion from an elevated line source: measurements of wind-concentration moments and budgets, J. Fluid Mech. 136 (1983) 111–137.
[12] R. Smith, Time-dependent releases of solute in parallel flows, J. Fluid Mech. 195 (1988) 587–595.
[13] P.J. Sullivan, H. Yip, A solution-scheme for the convective-diffusion equation, Z. Angew. Math. Phys. 36 (1985) 596–608.
[14] P.J. Sullivan, H. Yip, Near-field contaminant dispersion from an elevated line-source, Z. Angew. Math. Phys. 38 (1987) 409–423.
[15] P.J. Sullivan, H. Yip, Near-source dispersion of contaminant from an elevated line-source, Z. Angew. Math. Phys. 40 (1989) 297–299.
[16] P.J. Sullivan, H. Yip, Contaminant dispersion from an elevated point-source, Z. Angew. Math. Phys. 42 (1991) 315–318.
[17] G.I. Taylor, The dispersion of matter in turbulent flow through a pipe, Proc. Roy. Soc. London A 223 (1954) 446–468.